Experiment and Simulation of Laser Effect on Thermal Field of Porcine Liver

K.Ting, K. T. Chen, Y. L. Su, C. J. Chang

Abstract—In medical therapy, laser has been widely used to conduct cosmetic, tumor and other treatments. During the process of laser irradiation, there may be thermal damage caused by excessive laser exposure. Thus, the establishment of a complete thermal analysis model is clinically helpful to physicians in reference data. In this study, porcine liver in place of tissue was subjected to laser irradiation to set up the experimental data considering the explored impact on surface thermal field and thermal damage region under different conditions of power, laser irradiation time, and distance between laser and porcine liver. In the experimental process, the surface temperature distribution of the porcine lever was measured by the infrared thermal imager. In the part of simulation, the bio heat transfer Pennes's equation was solved by software SYSWELD applying in welding process. The double ellipsoid function as a laser source term is firstly considered in the prediction for surface thermal field and internal tissue damage. The simulation results are compared with the experimental data to validate the mathematical model established here in.

Keywords—laser infrared thermal imager, bio-heat transfer, double ellipsoid function.

I. INTRODUCTION

THE rapid development and progress of laser technology has made application in medical areas more and more extensive, such as cancer tumor heating therapy, cosmetic laser therapy etc.. In order to avoid necrosis of good tissues caused by excessive thermal energy during the process of *in vivo* laser surgery, the prediction of temperature distribution is very critical.[1]-[8].

Pennes's heat transfer equation was widely implemented to study the thermal effect of laser-tissue interaction [9]-[11]. In solving this bio-heat transfer equation, Beer's model which only considering the effect of laser light absorbed by tissues [12], [13].was often used to describe the behavior of laser heat source term. Both scattering [14]-[16] and thermal diffusion two effects are taken into account, the equation will become increasingly complex [17]. In bio-heat transfer issue, laser energy is instantaneously applied to one region, and this energy resulted significant energy change in the region, this situation is similar to welding heat transfer issue, therefore, it is feasible to use welding heat source in bio-heat transfer issue.

K. Ting is with the Graduate School of Engineering Technology, Lunghwa University of Science and Technology,No.300,Sec.1,Wanshou Rd.,Guishan Shiang,Taoyuan County 33306,Taiwan (R.O.C.) (e-mail: kuenting@mail.lhu.edu.tw).

K. T. Chen, is with the Department of Applied Mathematics, National Chung Hsing University, 250 Kuo Kuang Rd., Taichung 402, Taiwan R.O.C.(e-mail: ktchen@amath.nchu.edu.tw).

Y. L. Su, is with the Department of Applied Mathematics, National Chung Hsing University, 250 Kuo Kuang Rd., Taichung 402, Taiwan R.O.C.(e-mail: guthykimo@hotmail.com).

C. J. Chang is with the Chang Gung Aesthetic Medical Center, 2F., No.123, Dinghu Rd., Guishan Township, Taoyuan County 333, Taiwan (R.O.C.) (e-mail:chengjen@adm.cgmh.org.tw).

While simulating welding heat source in 1984, Goldak [18] developed a double ellipsoid heat source model, its advantage is that it is quite easy to change its heat source model and has versatility and flexibility. But Goldak ignored the effect of solid-liquid interface, did not take into account the impacts of molten zone and heat affect zone on thermal field, these two zones represent the regions of metal changed from solid state to liquid state and the region where phase change occurs. Double ellipsoid heat source model can correct the effect of molten pool or heat affect zone through the adjustment of Gaussian parameters [19], [20], and it is a method that has been adopted by many researchers in welding analysis. Rajan [12] used bio-heat transfer equation to calculate the latent heat to simulate phase-change (phase change temperature is 100ºC) of tissues, and assumed regions of occurring phase change phenomena of vaporization, melting as the equivalence as heat affect zone of welding. Laser has characteristics of strong penetration ability on tissues, the energy density distribution of rear half part is larger than the energy density distribution of front half part while laser acting on tissues, double ellipsoid function can change energy density distribution trend by adjusting Gaussian parameters, so that simulation result is closer to real situation. However, it is required to adjust more parameters when using double ellipsoid heat source function as laser heat source term, so in this study at first made adjustment on Gaussian parameters in ellipsoid function and thermal efficiency. Currently, Nd: YAG laser and diode laser are often used in inner layer skin laser treatment process, such as for hemangioma and vascular malformation [21], [22], the wavelength range of diode laser is 800 to 940nm, its penetration depth can be up to 3~4mm [23]. This study adopted experiment and simulation methods to get thermal field of tissues acted by laser diode. In the part of experiment, porcine liver with more uniform tissue swas conducted experiment, while the required thermal parameters used in numerical calculations referenced the results of Watanabe [24]. Finally, we explored thermal fields of surface and internal tissues under conditions of different power, laser irradiation time, and distance between laser and the surface of porcine liver.

II. EXPERIMENTAL METHOD

The main factors that affect the thermal behaviors of porcine liver are power and irradiation time, and the location of the laser under the tissues. According to clinical experience of physicians, the power used in the therapy is 10W, laser irradiation time is about 10s/per time and the distance between laser and the surface of porcine liver is about within the range of 1cm.In this study, the experiments were arranged under the conditions of power of (5W, 10W, 15W), laser irradiation time of (10s, 15s, 20s) and distance between laser and the surface of

World Academy of Science, Engineering and Technology
International Journal of Physical and Mathematical Sciences
Vol:6, No:5, 2012

porcine liver of (3mm, 5mm, 7mm).There were5 experiments corresponding to each set of parameters as shown in Table I. Fig. 1 shows the schematic diagram of the experiment. The tissue of porcine liver is soft with irregular shape. Thus the liver samples were cut into cubes with length and width of 20mm(length)× 20mm(width)×(15~20mm)(high) and inserted into acrylic cube box as shown in Fig. 2.
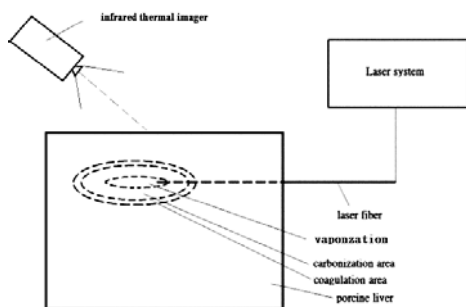
Fig. 1 Schematic diagram of conducting the experiment
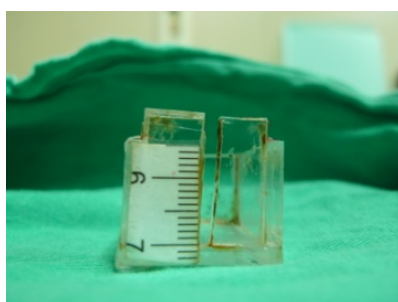
Fig. 2 Cubic box used in the experiment

TABLE I
EXPERIMENTAL CONDITIONS WITH SINGLE CONDITION CHANGED

Experimental condition	Range of exploration
Power (Watt, W)	5W, 10W, 15W
Laser irradiation time (second, s)	10s, 15s, 20s
Distance between laser and the surface of porcine liver (mm)	3mm, 5mm, 7mm

The infrared thermography of ThermaCAM^{TM} S60of FLIR Systems Company was used to detect surface thermal fields from laser starting point to the stopping point during the diode laser of DIOMED 15 irradiated to the porcine liver interior. The damage volume of the porcine lever due to the excessive heat was also measured as shown in Fig. 3.

Fig. 3 Measure of damage volume and infrared thermography

III. THEORETICAL BASIS

A. Heat transfer equation and mesh model

Pennes's bio-heat transfer equation was widely used to study the thermal interaction effects between laser and tissue and can be expressed as follows:

$$k\nabla^2 T + \rho_b C_b \omega_b (T_a - T) + Q_m + Q_r = \rho C_p \frac{\partial T}{\partial t} \quad (1)$$

Where k, ρ, and $C_p$are the thermal transfer coefficient, density, specific heatof the tissues;ρ_b, C_p, and $\omega_b$are density, specific heat, and blood instill rate of blood veins；and Q_m, Q_r, and $T_a$are metabolic rate, laser heat source term, and arterial blood temperature of the tissues. As the porcine liver used in the experiment is not in *vivo*, so the influences of flow of blood and metabolism of tissues on temperature are very small, so Eq.(1) can be simplified into:

$$k\nabla^2 T + Q_r = \rho C_p \frac{\partial T}{\partial t} \quad (2)$$

Sysweld software is finite element analysis software developed by ESICompany [25], its main function is for handling phase change generated in welding and calculating residual stress and temperature produced by welding. While in the establishment of the grid model, the Company has developed a more user-friendly subsidiary software Visual mesh operated in Visual environment, it can be used to perform various functions, such as combining elements and nodes between objects and simplify modeling procedure; when Visual mesh is used in model with more complex geometries, it has more user-friendly functions for easily and quickly constructing a model.

Considering the geometric model of porcine liver as an axisymmetric rectangular model with dimension of 20mm × 10mm × 20mm, Fig.4 shows the mesh model of porcine liver. The model has a total of 18,000 elements, and a total of 6,057 nodes.
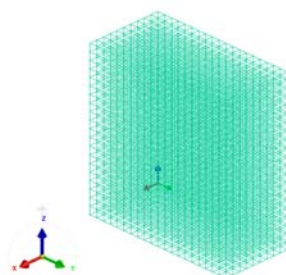

Fig. 4 The mesh model of porcine liver

B. Laser heat source

In analyzing of bio-heat transfer, Yilba [26] proposed a 1-D heat source model to solve 1-D thermal field issue. And Fanjul [27] proposed a 3-D heat source model for solving 3-Dthermal field issue, the heat source function can be expressed as:

$$Q_r = \mu_a I_0 e^{-\mu_a z} e^{-s(x^2 + y^2)} \quad (3)$$

where s is laser beam radius, μ_a (mm^{-1}) is absorption coefficient, andI_0 (W/mm^2) is laser intensity. This study used double ellipsoid heat function to simulate laser light source based on the theory firstly proposed by Rosenthal in 1940 [28].The drawback was that the thermal field near heat source to be

World Academy of Science, Engineering and Technology
International Journal of Physical and Mathematical Sciences
Vol:6, No:5, 2012

distorted. Pavelic [29] in 1960 proposed a plane Gaussian heat source mathematical model that heat energy distribution in a round plate is Gaussian distribution to solve Rosenthal' problem. And in 1984, Goldak proposed double ellipsoid heat source function, this function considers that the temperature gradient in the front half part of heat source is changed more largely than that in the rear half part, (4) represent power density of the front and rear half parts of heat source respectively.

$$Q_{r_f}(x,y,z,t) = \frac{6\sqrt{3}Q_f}{abc_f\pi\sqrt{\pi}} e^{-3\left(\frac{x^2}{a^2} + \frac{y^2}{b^2} + \frac{[z+v(\tau-t)]^2}{c_f^2}\right)} \tag{4}$$

$$Q_{r_r}(x,y,z,t) = \frac{6\sqrt{3}Q_r}{abc_r\pi\sqrt{\pi}} e^{-3\left(\frac{x^2}{a^2} + \frac{y^2}{b^2} + \frac{[z+v(\tau-t)]^2}{c_r^2}\right)}$$

where a, b, c_f, and c_r are Gaussian parameter terms; v, τ are the welding rate and time respectively for moving heat source arrived to given position ξ; and $\xi = z + v(\tau - t)$; Q_f, Q_r are maximum heat powers, their calculation methods are shown as below:

$$Q_f = f_f Q, \; Q_r = f_r Q, \; Q = VI\eta \tag{5}$$
$$f_f + f_r = 2$$

f_f and f_r respectively denotes the heat deposit of front half part and rear half part, the relationship between the two coefficients must satisfy (5),V, I, and η represent voltage, current, and thermal efficiency.Fig.5 shows that the power density distribution function corresponding to various laser sources can be achieved by adjusting the Gaussian parameters.
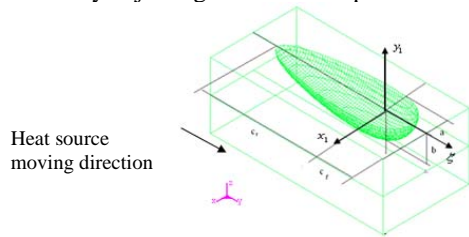

Fig. 5 Double elliptic function model

In simulation, consider heat source acts on a single point and both f_f and f_r are set to 1, adjust the Gaussian parameters a, b, c_f, c_r and thermal efficiency η to find out a set of parameters in line with the diode laser, and then conduct surface thermal field simulations respectively for power, laser irradiation time, distance changes between laser and the surface of porcine liver.

C. Material parameters

Assume tissues within porcine liver are uniformly distributed, and ignore major liver blood vessels and holes of capillaries within the porcine liver, then the tissues could be considered as a homogeneous material. Thermal transfer coefficient, specific heat, density parameters refer to the results obtained by Watanabe:

$$c_{liver} = a_1 T_{liver} + b_1$$
$$k_{liver} = a_2 T_{liver} + b_2 \tag{6}$$

where c_{liver} is specific heat of porcine liver,$k_{liver}$is thermal conductivity of porcine liver and T_{liver} is temperature of porcine liver, a_1 =3.2 J/kgK^2, b_1 =3.2×10^3 J/kgK, a_2

=9.2×10^{-3} W/mK^2 and b_2 =1.2×10^{-1} W/mK. Density is 1060 kg/m^3.

D. Initial conditions and boundary conditions

Considering that the initial temperature of porcine liver is at room temperature, expressed as

$$T(x,y,z,0) = 25℃ \tag{7}$$

Plane of symmetric axis is insulation; equation (8) indicates the mathematical formula of boundary conditions of natural convection and radiation.

$$k\frac{\partial T}{\partial n} = h(T - T_\infty) + \sigma\varepsilon(T^4 - T_\infty^4) \tag{8}$$

where heat convection coefficient h = 10 W/mm^2 K, ambient temperature T_∞= 25℃, Boltzmann constant σ = 5.76×10^{-8}W/m^{2}K^4, emissivityε = 0.8。

IV. RESULTS AND DISCUSSIONS

A. Surface thermal field distribution of adjusting Gaussian parameters

When double ellipsoid Gaussian function is used to simulate laser heat source, surface thermal field distribution due to diode laser surgery can be obtained by adjusting Gaussian parameters and thermal efficiency. The position of surface thermal field of heat center is at coordinates (0, 10, 20) shown in Fig.6, and the position on which of the laser acts on under the surface of porcine liver. Experimental condition is fixed 10W10s3mm.Fig. 7 shows the surface temperature curve around the center of heat source and along x-axis direction. The Gaussian parameters combination used are$a=b=1$, $c_f=c_r=7$ and thermal efficiency to be 0.15.This figure shows the maximum surface temperature is about 38℃, and the change of surface temperature is 16℃..
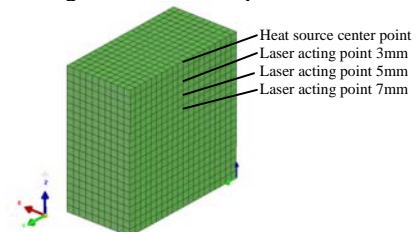

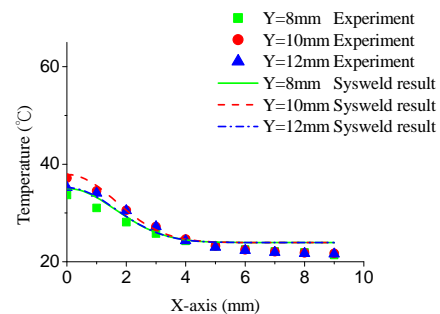Fig. 6 Schematic diagram of laser heat source acting position

Fig. 7 Surface temperature curve of 10W10s3mm around heat source along X-axis

B. Surface thermal field distribution of different powers

After the adjustments of Gaussian parameters and thermal efficiency of laser diode obtained in previous section, then the

World Academy of Science, Engineering and Technology
International Journal of Physical and Mathematical Sciences
Vol:6, No:5, 2012

surface thermal fields can be calculated under fixed irradiation time, and 3mm distance between laser and surface of porcine liver at different powers. Fig.8 shows the surface temperature curve around the heat source center along X-axis direction under different powers. It shows that values of maximum surface temperature power are 27ºC, 38ºC and 47ºC corresponding to the power 5W, 10W and 15W. The maximum surface temperature is increasing with power increase and surface temperature rising rate is highest at 10W. Fig. 9 shows the surface thermal field distribution of different powers by Sysweld.
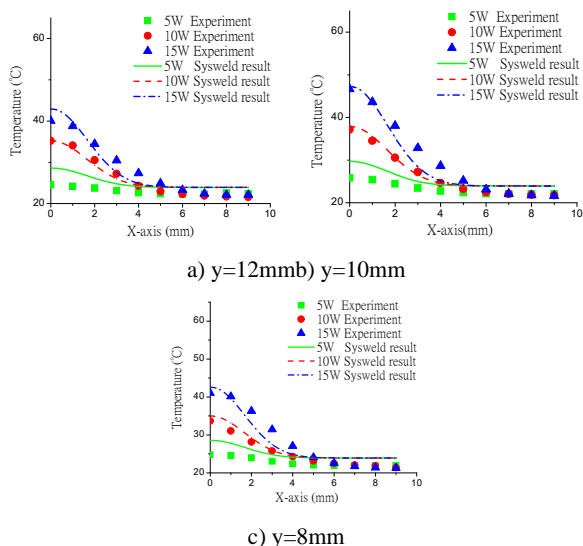

a) y=12mmb) y=10mm

c) y=8mm

Fig. 8 Surface thermal field curve along X-axis at a) y=12mm b) y=10mm c) y=8mm under different powers
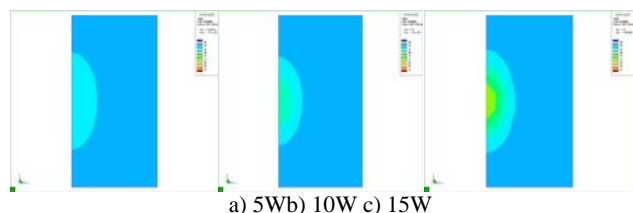

a) 5Wb) 10W c) 15W

Fig. 9 Surface thermal field distribution by Sysweld under different powers

C. Surface thermal field distribution of different laser irradiation times

When the power is fixed at 10W, and distance between laser and surface of porcine liver is fixed at 3mm, Fig. 10 shows surface temperature curve under different laser irradiation times. When the time is 10 seconds, the maximum surface temperature is about 38ºC with an increase of 16ºC.And when the time increased from 10s to 15s, the surface temperature again increased about 16ºC, and the maximum temperature then is 54ºC.When the time is increased from the 15s to 20s, the temperature at the center of heat source increased by 6ºC, the maximum temperature then is 60ºC.

From these results, it can be known that as laser irradiation time becomes longer, the surface temperature will rise fast in the beginning and will slow down after 15 seconds. Fig. 11

shows surface thermal field distribution and thermal image map under different laser irradiation times.
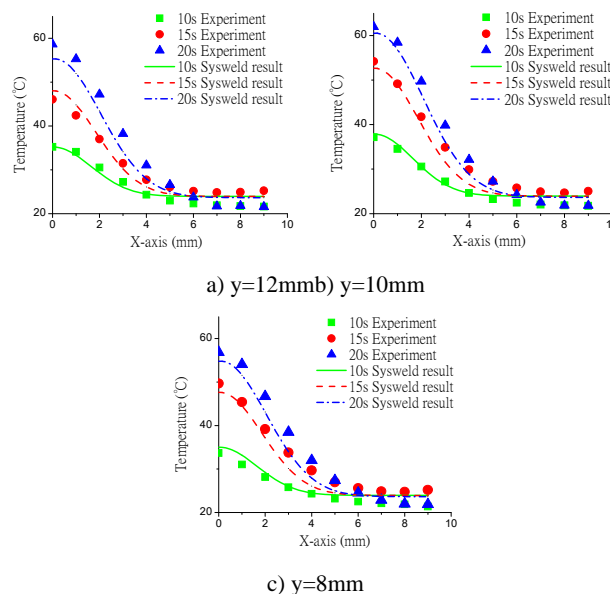

a) y=12mmb) y=10mm

c) y=8mm

Fig. 10 Surface thermal field curve along X-axis at a) y=12mm b) y=10mm c) y=8mm under different laser irradiation times
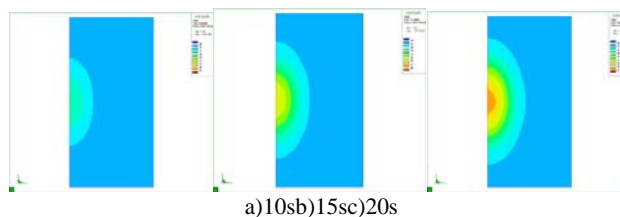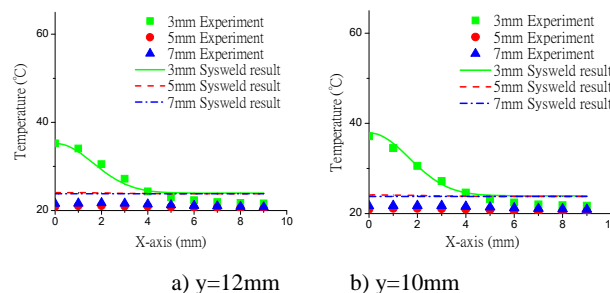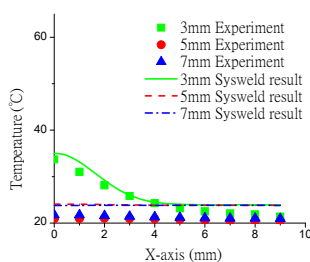

a)10sb)15sc)20s

Fig. 11 Surface thermal field distribution by Sysweld under different laser irradiation times

D. Surface thermal field distribution of different distances between laser and the surface of porcine liver

The impact of distance between laser and the surface of laser on surface thermal field mainly comes from radial energy of laser and heat transfer within the tissues. Fig. 12 shows surface temperature curve under different distances between laser and the surface of porcine liver when laser power, irradiation time are fixed at 10W, 10s respectively. When the distance between laser and the surface and porcine liver is greater than 5mm, the surface temperature is almost no significant of change. Fig. 13 shows surface thermal field distribution by Sysweld under different distances between laser and surface of porcine liver.

a) y=12mm   b) y=10mm

World Academy of Science, Engineering and Technology
International Journal of Physical and Mathematical Sciences
Vol:6, No:5, 2012

c) y=8mm

Fig. 12 Surface thermal field curve along X-axis at a) y=12mm b) y=10mm c) y=8mm under different distances between laser and surface of porcine liver
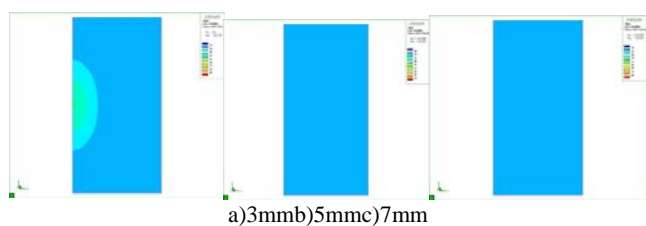
a)3mmb)5mmc)7mm

Fig. 13 Surface thermal field distribution by Sysweld under different distances between laser and surface of porcine liver

E. Thermal damage within the tissues

To establish the accurate heat transfer model for the tissues of porcine liver, the thermal damage can also be used to calibrate. In this experiment, the categories of main thermal damage of tissue are coagulation and carbonization. The criterion of the coagulate and carbonized zone can be assumed as the reach values of 60℃ or over 100 ℃ .Fig.14 indicates that the trend of thermal damage is linear increasing with power 5W~15W, damage volume increased about 90 mm^3. And when laser irradiation time is within the range of 10s~20s, the trend of increased thermal damage volume is also in linear to increase of about 110mm^3. While thermal damage volume has not changed significantly under different distances between laser and surface of porcine liver. Fig.15-17 respectively shows simulation results under different powers, laser irradiation times, and different distances between laser and surface of porcine liver. In the simulation results, green and red areas represent the coagulation and carbonization zone respectively.

V. CONCLUSIONS

In this paper, the double ellipsoid function was successfully to simulate bio-heat transfer model during diode laser irradiation through the verifications of the measurements of surface temperature and thermal damage zone.

The adjustments of Gaussian parameters and thermal efficiency, *a=b=1, c$_f$=c$_r$=7*, thermal efficiency is 0. 15, the characteristics of diode laser can be correctly described.

When power of diode laser is within the range of 5W~15W, irradiation time is 10s, and the distance between laser and surface of porcine liver is 3mm, the maximum surface temperature is 27~47ºC.

When irradiation time of diode laser is within the range of 10s~20s, power is 10W, and the distance between laser and probe is 3mm, the maximum surface temperature is 37~60ºC.
When the distance between laser and surface of porcine liver is

3~7mm, power is 10W, and irradiation time is 10s, no change in surface temperature from exceeding 3mm.
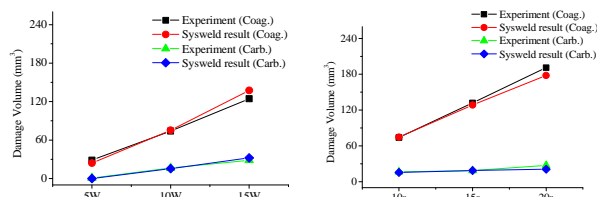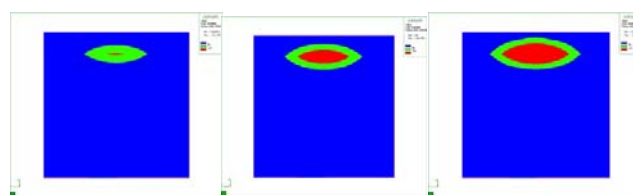

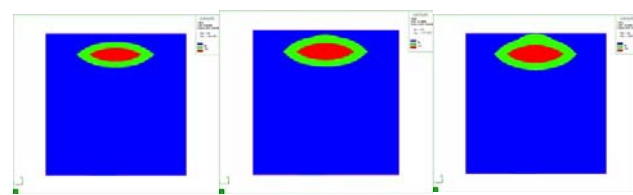a) Different powers   b)Different laser irradiation times
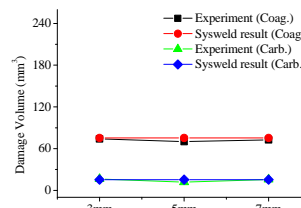
c) Different distances between laser and surface of porcine liver
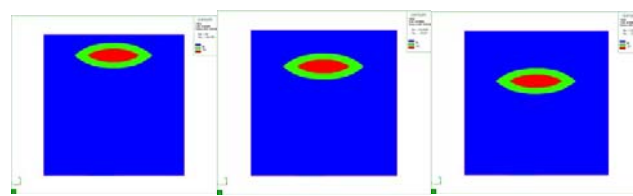Fig. 14 Thermal damage volume under different conditions

a) 5Wb)10Wc) 15W

Fig. 15 Numerical simulation results of damage under different powers

a) 10sb) 15sc) 20s

Fig.16 Numerical simulation results of damage under different laser irradiation times

When applying laser in clinical surgery, if power is below 10W and laser irradiation time is less than 10s, it is recommended that the laser depth is not less than 5mm, to avoid thermal damage in surface of tissues caused by increase of surface temperature.

a) 3mm b) 5mmc)7mm
Fig. 17 Numerical simulation results of damage under different distances between laser and surface of porcine liver

Thermal damage volume within tissues of porcine liver

World Academy of Science, Engineering and Technology
International Journal of Physical and Mathematical Sciences
Vol:6, No:5, 2012

under different irradiation times is about within the range of 60~180mm^3; thermal damage volume under different powers is about within the range of 30~120mm^3; while in changing distance between laser source and the surface of porcine liver, the thermal damage volume is almost no change.

REFERENCES

[1] K. Ivarsson, J. Olstrud, C. Sturesson, et al, Feedback interstitial diode laser (805 nm) thermotherapy system: ex vivo evaluation and mathematical modeling with one and four-fibers, Lasers in Surgery and Medicine 22: 86–96 (1998).

[2] A.M. Minhaj, F. Manns, P.J. Milne, et al, Laser interstitial themotherapy (LITT) monitoring using high-resolution digital mammography: theory and experimental studies, Physics in Medicine and Biology 47: 2987–2999 (2002).

[3] E. Rohde, I. M. V. Rheinbaben, A. Roggan, et al, Interstitial Laser-Induced Thermotherapy (LITT): Comparison of In-Vitro Irradiation Effects of Nd:YAG (1064 nm) and Diode (940 nm) Laser, Medical Laser Application. 16: 81–90 (2001).

[4] A. Roggan, J. P. Ritz, V. Knappe, et al, Radiation Planning for Thermal Laser Treatment, Medical Laser Application 16: 65–72 (2001).

[5] V. Knappei, A. Roggan, M. Glotz, et al, New Flexi ble Applicators for Laser-Induced Thermotherapy, Medical Laser Application 16: 73–80 (2001).

[6] R. A. London, M. E. Glinsky, G. B. Zimmerman, Laser–tissue interaction modeling with LATIS, Applied Optics 36：9068-9074 (1997)

[7] R. A Thomas, K. E Donne, M. Clement, et al, Ther- mographic Methods During Laser-Tissue Interaction

[8] A. M. MOLS, V. KNAPPE, H. BUHR, Laser-induced Thermo- therapy (LITT): Dose-Effect Relation on Lung Tissue Medical Laser Application19:160-166 (2004)

[9] H. H. Pennes, Analysis of tissue and arterial blood temperatures in the resting human forearm. Journal of Applied Physiology 1: 93–122 (1948).

[10] B. X. Wang and Y. M. Wang, study on the basic equations of biomedical heat transfer, Transport Phenomena Science and Technology: 273-276 (1992).

[11] S. F Cheng, Bio-heat heat transfer analysis of elective photocoagulation method coordinated with jet cooling effect, Department of Applied Mathematics, National Chung Hsing University, PhD dissertation (2007).

[12] S. Karaa, J. Zhang, F. Yang, A numerical study of a 3D bioheat transfer problem with different spatial heating, Mathematics and Computers in Simulation 68: 375 -388 (2005).

[13] W. Shen, J. Zhang, Modeling and Numerical Simulation of Bioheat Transfer and Biomechanics in Soft Tissue, Mathematical and Computer Modelling 41: 1251- 1265 (2005).

[14] G. Yoon, A. J. Welch, M. Motamedi, et al, Develop- ment and Application of Three- Dimensional Light Distribution Model for Laser Irradiated Tissue, IEEE Journal of Quantum Electronics 23: 1721-1733 (1987).

[15] G. L. LeCarpentier, M. M. Linda, P. McMath, et al, Continuous Wave Laser Ablation of Tissue: Analysis of Thermal and Mechanical Events, IEEE Tran- sactions on Biomedical engineering 40: 188-200 (1993).

[16] F. F. Vélez, O. G. Romanov, J. L. A. Diego, Efficient 3D numerical appro- ach for temperature prediction in laser irradiated biological tissues, Computers in Biology and Medicine 39: 810 – 817 (2009).

[17] R. Dua, S. Chakraborty, A novel modeling and simulation technique of photothermal interactions between lasers and living biological tissues under- going multiple changes in phase, Computers in Biology and Medicine 35: 447-462 (2005).

[18] J. Goldak, A. Chakravarti, M. Bibby, A new finite element model for welding heat sources. Metallurgical Transactions B 15B: 299-305 (1984).

[19] K. Abderrazak, S. Bannour, H. Mhiri, Numerical and experimental study of molten pool formation during continuous laser welding of AZ91 magnesium alloy, Computational Materials Science 44：858–866 (2009).

[20] S.A. Tsirkas, P. Papanikos Th. Kermanidis, Numerical simulation of thw laser welding process in butt-joint specimens, Journal of processing Technology 134：59-69 (2003).

[21] M. K. Sidhu, A. J. Perkins, W.W. Shaw Dennis, M. A. Bittles,et al, Mhiri, Ultrasound-guided Endovenous Diode Laser in the Treatment of Congenital Venous Malformations: Preliminary Experience, Journal of Vascular and Interventional Radiology 16 : 879-884(2005).

[22] P. Lanzetta, G. Virgili, E. Ferrari, Diode laser photo -coagulation of choroidal hemangioma,International Ophthalmology 19: 239-247(2004)

[23] J. G. Eichler, O. Goncalves, A Review of Different Lasers in Endonasal Surgery :Ar-, KTP-, Dye-, Diode-, Nd-, Ho- and CO2-Laser , Medical Laser Application 17: 190–200 (2002)

[24] H. Watanabe, Y. Kobayashi, T. Hoshi, et al, Integrated System for RFA Therapy with Biomechanical Simulation and Needle Insertion Robot,System Integration, IEEE/SICE International Symposium on :54-59 (2009)

[25] N.Siva Shanmugam , G. Buvanashekaranb, K. Sankaranarayanasamy, etc, A transient finite element simulation of the temperature and bead profiles of T-joint laser welds, International Journal of Modelling and Simulation 30: 5168- 5183(2010)

[26] B. S. Yilbas, Z. Yilbas, M. Sami, Thermal processes taking place in the bone during CO^2 laser irradiation, Optics & Laser Technology 28: 513 -519 (1996)

[27] G. L. LeCarpentier, M. M. Linda, P. McMath, et al, Continuous Wave Laser Ablation of Tissue: Analysis of Thermal and Mechanical Events, IEEE Transactions on Biomedical engineering 40: 188- 200 (1993).

[28] D. Rosenthal, Mathematical theory of heat distrib- ution during welding and cutting, Transaction of the ASME 43: 849-866 (1946).

[29] V. Pavelic, R. Tanbakuchi, O. A. Uyehara, et al, Welding Journal Research Supp- lement 48: 295- 305 (1969).